

Rational Design of Improved Aziridine-Based Inhibitors of Cysteine Proteases

Verena Buback,[†] Milena Mladenovic,[‡] Bernd Engels,[‡] and Tanja Schirmeister^{*,†}

Institut für Pharmazie und Lebensmittelchemie, Institut für Organische Chemie, Universität Würzburg, Am Hubland, D-97074 Würzburg, Germany

Received: December 1, 2008; Revised Manuscript Received: February 7, 2009

Quantum chemical computations on appropriate model systems are used for a rational design of aziridine-based inhibitors of cysteine proteases. They predict that already inductive electron-withdrawing substituents at the aziridine nitrogen strongly accelerate the alkylation step of the inhibition process in neutral and alkaline media, but also for more acidic environments improvements are predicted. With this we generalize previous findings that found similar effects for N-formylated compounds. Furthermore, the new substituents possess the additional advantage that they do not open up reaction pathways other than the nucleophilic ring opening. To verify the hypotheses selected compounds were synthesized and tested. These tests approved the predictions and showed that the corresponding derivatives of aziridine-2,3-dicarboxylate are potent irreversible inhibitors of cysteine proteases. On the basis of measured inhibition data the new inhibitors offer an up to 2,300-fold increase in inhibition potency compared to the unsubstituted inhibitor. Additionally, the kinetics of a selected reaction with 4-methoxy thiophenolate as model thiol were measured in solution to ascertain that the inhibition mechanism is the irreversible alkylation of the cysteine residue of the protease's active site under ring opening of the new inhibitors.

Introduction

According to the World Health Organization (WHO), 25% of all cases of death worldwide are caused by infectious diseases.¹ Among them, tropical diseases such as malaria, leishmaniosis, or the African trypanosomiasis (sleeping sickness) are of extreme importance, since no appropriate vaccines exist so far. Cysteine proteases, especially those of the papain family (clan CA, family C1)² play important roles in the life cycles of the parasites that cause these tropical diseases.^{3–5} Therefore, the rational design of cysteine protease inhibitors as new drug candidates is an important step in combat against these infections.

The active site of papain-like cysteine proteases consists of a catalytic dyad of cysteine and histidine, existing as an ion pair in which the catalytic His has been protonated by the catalytic Cys prior to substrate binding.^{6–8} Irreversible alkylation or acylation of the negatively charged cysteine thiolate residue of the protease's active center leads to inactivation of cysteine proteases. Naturally occurring epoxysuccinyl peptides, for example, E-64c from *Aspergillus japonicus*,⁹ have been identified as potent cysteine protease inhibitors. The mode of action of epoxide-based inhibitors is commonly described as a two step mechanism (Scheme 1). The presence of a trans-configured epoxysuccinic acid moiety is crucial for the inhibition, since in the first step it assures a favorable arrangement of the inhibitor within the binding pocket, leading to a noncovalently bonded enzyme inhibitor complex EI. The efficiency of the first step is characterized by the dissociation constant K_i of the noncovalent enzyme inhibitor complex EI. In the second step of the inhibition process, the epoxide ring is opened when attacked at one of the ring carbon atoms, resulting in irreversible alkylation of the Cys-residue of the enzyme's active site (E-I). The efficiency of

SCHEME 1: Two-Step Model for the Irreversible Inhibition of Cysteine Proteases; E = Enzyme; EI = Noncovalent Enzyme-Inhibitor Complex; E-I = Covalently and Irreversibly Blocked Enzyme



this second step is characterized by the first-order rate constant of inhibition k_i .

Since often no information about the two single steps is available, the overall inhibition potency of an irreversible inhibitor is also characterized by k_{2nd} , which is the quotient of k_i and K_i ($k_{2nd} = k_i/K_i$).

In the style of epoxysuccinyl peptides, aziridinyl peptides, among them notably derivatives of trans-aziridine-2,3-dicarboxylic acid, have also been introduced as effective cysteine protease inhibitors during the last decades.^{10–13} In spite of the common principal inhibition mechanism, several differences can be found between epoxides and aziridines including alkylation rates and the influence of the medium and substituent effects. Contrary to epoxides, aziridines feature an additional substitution site at the nitrogen atom, offering interesting possibilities to modulate the inhibitors reactivity without replacing the already existing substituents. The attachment of enzyme affinity-enhancing peptide sequences or the targeted introduction of markers (such as biotin)^{14,15} or functional groups to study reaction mechanisms are valuable applications.

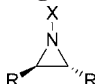
The inhibition potency of epoxide- and aziridine-based agents depends differently on the pH-value of the environment. In neutral and alkaline media, epoxide-based inhibitors have higher potencies than the aziridine counterparts. In acidic environment aziridine-based inhibitors feature reactivities that are similar to those of the epoxide derivatives.¹⁰ Previous quantum chemical calculations^{16,17} regarding the ring-opening reaction of the three-membered heterocycles aziridine, oxirane, and thiirane with the nucleophile methylthiolate representing the cysteine residue of

* To whom correspondence should be addressed. E-mail: schirmei@pharmazie.uni-wuerzburg.de. Phone: ++49(0)9318885440.

[†] Institut für Pharmazie und Lebensmittelchemie, Universität Würzburg.

[‡] Institut für Organische Chemie, Universität Würzburg.

TABLE 1: Inhibitors Investigated in the Present Work



inhibitor	X	R	ref/remark
1	CHO	CO ₂ Et	18
2	H	H	18
3	CHO	H	18
4	Cl	H	computed
5	Br	H	computed
6	CF ₃	H	computed
7	CF ₂ H	H	computed
8	C ₆ H ₄ NO ₂	H	computed
9	Cl	CO ₂ Et	synthesized, tested
10	Br	CO ₂ Et	synthesized, tested
11	CF ₂ CO ₂ Et	CO ₂ Et	synthesized, tested
12	H	CO ₂ Et	47
13	CH ₂ CO ₂ Et	CO ₂ Bn	47

the protease's active site explained these trends by the different influence of acidic media on kinetics and thermodynamics of the corresponding ring-opening reactions. For aziridine-based inhibitors, already a weak or medium acidic environment leads to a protonation of the nitrogen center at the beginning of the reaction course. This stabilizes transition state and product of the ring-opening reaction. As a consequence, the reaction rate is significantly enhanced in comparison to nonprotonated aziridine compounds and the reaction becomes irreversible due to the product stabilization. For epoxide-based inhibitors the protonation of the oxygen center takes place after the transition state, that is, only the product is strongly stabilized while the kinetics remains unchanged.

The studies underlined that many differences between epoxide- and aziridine-based inhibitors can be correlated with the ability of the heteroatoms to stabilize the charge that accumulates in the course of the ring-opening reactions. Hence, electron-withdrawing substituents at the nitrogen atom should lead to lower reaction barriers of aziridines and in turn to higher inhibition potencies. Keeping in mind that N-acylated derivatives are in general more potent than the corresponding N-unsubstituted or N-alkylated derivatives,^{11–13} in a first attempt to obtain improved aziridine-based inhibitors the potency of N-formylated compounds was studied (inhibitor 3, Table 1).¹⁸ Quantum chemical calculations predicted that the attachment of a CHO-group at the N-position of the aziridine ring should lower the reaction barrier for nucleophilic attack by methylthiolate by about 14 kcal mol⁻¹. This indicates that N-formylated derivatives possess increased potencies since the k_i values of the second step of the inhibition process are enhanced. Measurements for N-formylated aziridine-2,3-dicarboxylate **1** (Table 1),¹⁸ which was synthesized and tested in fluorometric assays on the CAC1² cysteine protease cathepsin L and related proteases, for example, the cathepsin-L-like protease falcipain 2 from *Plasmodium falciparum*,¹⁹ indeed proved an increase in k_{2nd} by a factor of 3500 but surprisingly due to an improved K_i -value and not an increased k_i -value. Continuing computations¹⁸ could clarify these unexpected findings. They showed that the attack of the cysteine moiety at the carbonyl group of the CHO-substituent possesses a much lower barrier than the corresponding attack at the ring-carbon. However, this second reaction is endothermic, that is, the formed complex will decompose on a fast time scale. Such reversible formylation reactions are known for peptidyl aldehydes.²⁰ An enhanced K_i -value results due to multiple formation and decomposition of a reversible complex before the ring-opening reaction finally leads to an irreversibly blocked enzyme.

The decrease of the reaction barrier of the irreversible ring-opening reaction is in this case perhaps not reflected in k_{2nd} since both reactions influence each other.

Substitution of the carbon positions of the aziridine ring with fluorine, chlorine, or bromine also led to spectacularly elevated rates of ring cleavage reactions.^{21,22} But also with such substitutions new reaction possibilities are opened that might decrease the inhibition potency.²²

Our first attempt advises that for an improvement of the potency on the basis of k_i substituents should be used that do not open up new reaction paths. Hence, in the present study we focus on substitution pattern at the nitrogen center with appropriate substituents. The potencies of various substituents selected on the basis of our previous results are investigated using quantum chemical approaches. For the best substituents, appropriate inhibitors are synthesized. Finally their inhibition potencies are tested and reactions with a model thiol are performed and followed by NMR-spectroscopy in order to measure the rate constants of the ring-opening reaction. The paper is arranged as follows: In the first part the computations are described. Subsequently, synthesis and measurements of the inhibition constants and reaction rates with the model nucleophile are discussed.

Model System and Computational Details

Models, which reliably describe enzyme inhibition processes, have to account for the influence of the protein and the solvent environment. This can be done with quantum mechanic/molecular mechanic (QM/MM) approaches that explicitly take into account enzyme and solvent. Such approaches were necessary to describe the regio-²³ and stereoselectivity²⁴ of the inhibition process of papain-like proteases by epoxide- or aziridine-based agents and to explain the influence of the catalytically relevant His-moiety of cysteine proteases.²⁵ However, often already pure QM computations for smaller model systems are extremely helpful.²⁶ For example, the effect of substituents, which are directly attached to the ring and that influence the inhibition process due to electronic reasons, could already be explained by a much simpler approach.^{16,17} This approach could also explain the pH-dependency of epoxide and aziridine-based inhibitors. It was even found to be accurate enough for predictions.¹⁸ This simplified model approximates the cysteine residue by a methyl thiolate. The environment is modeled either by two water molecules ($pK_a \approx 15$) to mimic a low proton-donating ability of the environment or two ammonium molecules ($pK_a \approx 9.3$) to simulate a higher one. They are employed in combination with the continuum model COSMO²⁷ ($\epsilon = 78.39$) that accounts for the overall polarizability of the solvent and the protein environment. Only the electrophilic warhead of the inhibitor and its direct substituents are taken into account. Information about the kinetics and thermodynamics of the irreversible step of the inhibition was obtained from potential energy surfaces of the inhibition process that were computed employing the B3-LYP/TZVP//BLYP/TZVP^{28–30} level of theory. Density functional theory (DFT) is well known to describe many properties with an excellent cost-benefit value.^{31–33} Nevertheless, this is often based on an error compensation that does not work in all cases,^{34–37} and indeed often multireference approaches are necessary to obtain reliable reaction paths.^{38–41} However, for the present problem the reaction paths computed with B3-LYP/TZVP//BLYP/TZVP closely resemble those obtained with higher level approaches.¹⁷

In the present work, the influence of several substitution patterns on the inhibition potencies of aziridine-based inhibitors

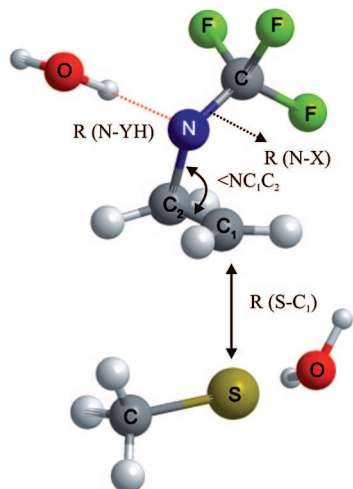


Figure 1. The notation for reaction coordinates and other geometrical parameters used in Table 2. The system with a CF_3 moiety as N-substituent ($\text{X} = \text{CF}_3$, inhibitor **6**, Table 1) and two water molecules as explicit solvent ($\text{Y} = \text{OH}$) are given as example.

has been tested. Since QM/MM computations would be prohibitively expensive, we used the simplified approach described above. To obtain a reliable description of the reactions two-dimensional PESs were computed by varying $\angle \text{NC}_1\text{C}_2$ and RC_1-S (Figure 1) independently. For each point of the two-dimensional PES, these reaction coordinates were kept fixed at certain values while all other internal degrees of freedom were optimized. Points close to the transition state on the PES then served as input for a numerical frequency analysis and subsequently a transition state (TS) search. The resulting TS structures were relaxed by a careful downhill optimization toward reactants and products to ensure that these stationary points were connected by contiguous paths. The geometries obtained in this process were used for the determination of barriers and reaction energies. The optimizations were done at the DFT/B-LYP/TZVP level of theory, while single-point calculations at the DFT/B3-LYP/TZVP level were performed to achieve more accurate relative energies. For all computations, the *TURBOMOLE*⁴² program package was used.

The influence of the electron-withdrawing substituents on the inhibition potency of aziridine-based inhibitors was estimated by quantum chemical calculations regarding the ring-opening reaction of substituted aziridines with methylthiolate (Scheme 2). For the rational design seven different substituents (H , CHO , Cl , Br , CF_3 , CF_2H , and $\text{C}_6\text{H}_4\text{NO}_2$) were tested. An enumeration of the resulting inhibitors is given in Table 1.

Syntheses, Enzyme Assays, and Model Reactions

To verify, the theoretical predictions inhibitors **9**, **10**, and **11**, which are the analogues of the computationally treated model compounds **4**, **5**, **6**, and **7**, were synthesized as follows. Reaction of diethyl aziridine-2,3-dicarboxylate **12**⁴³ with either *N*-chloro or *N*-bromo succinimide according to reference⁴⁴ yielded inhibitors **9** and **10**, respectively (Scheme 3). For the synthesis of inhibitor **11**, aziridine **12** was reacted with ethyl bromodifluoroacetate and sodium carbonate in acetone (Scheme 2).

The synthesis of an analog of the computationally treated inhibitor **8** failed. The kinetics and thermodynamics of the ring-opening reaction are thus discussed only from the theoretical point of view.

The inhibitors **9–11** were tested against the cathepsin L-like cysteine protease falcipain 2 from *Plasmodium falciparum* using

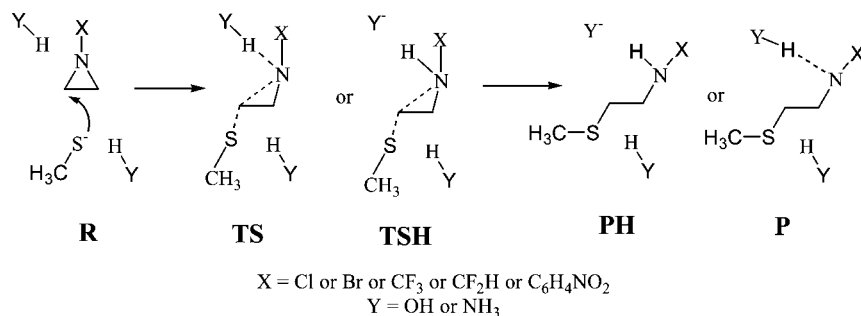
a standard fluorometric assay, as substrate Cbz-Phe-Arg-AMC was used which yields amino methyl coumarin (AMC) as fluorophor after cleavage of the substrate by the enzyme.¹³ A first screening with concentrations of $100\ \mu\text{M}$ was performed. Individual inhibition constants K_i , k_i , and $k_{2\text{nd}}$ were then determined in continuous assays according to the method described by Tian and Tsou by monitoring the product released from hydrolysis of the substrate in presence of the inhibitor as a function of time (fluorescence = $A(1 - \exp(-k_{\text{obs}}t)) + B$).⁴⁵ The fluorescence increase due to enzymatic hydrolysis of the substrate Cbz-Phe-Arg-AMC was measured over a period of ten minutes in the presence of inhibitor concentrations ranging from 10 to $1000\ \mu\text{M}$. DMSO was used as negative control. The pseudo first-order rate constants k_{obs} were then fitted against the inhibitor concentrations $[\text{I}]$ using the equation $k_{\text{obs}} = k_i[\text{I}]/(K_i^{\text{app}} + [\text{I}])$ yielding the apparent dissociation constant K_i^{app} and the first-order rate constant of inhibition k_i . The K_i^{app} value was corrected to zero substrate concentration by the term $(1 + [\text{S}]/K_m)$ in equation $K_i = K_i^{\text{app}}/(1 + [\text{S}]/K_m)$. The second-order rate constant $k_{2\text{nd}} = k_i/K_i$ was directly calculated from the individual constants. All constants were calculated by nonlinear regression analysis using the program GraFit.⁴⁶

Reactions of inhibitor **11** with the model thiol 4-methoxy thiophenol were performed and followed by NMR-spectroscopy as described earlier.¹⁸ The thiophenol used had served as a good model for the active site of cysteine proteases as it represents a rather acidic thiol ($\text{p}K_a = 7.4\text{--}7.8$) with half the concentration being deprotonated at the pH used (pH 7.6). In enzymatic assays and in vivo the ring-opening reaction shows pseudo first-order kinetics, whereas chemically the $\text{S}_{\text{N}}2$ ring-opening follows second-order kinetics. Therefore, the reaction of the aziridine **11** with 4-methoxy thiophenol was analyzed for varying concentrations of **11** (**11**, $0.008\ \text{mM}$ and $0.18\ \text{mM}$; thiol, $0.54\ \text{mM}$; $[\text{11}]/[\text{thiol}] = 1/9$ for pseudo first-order conditions or $1/3$ for second-order conditions).

Results and Discussions

Figures 2–6 give the computed potential energy surfaces for the inhibition reaction by the differently N-substituted aziridines (**4–8**, $\text{X} = \text{Cl}$, Br , CF_3 , CF_2H , and $\text{C}_6\text{H}_4\text{NO}_2$). Detailed data can be found in the Supporting Information. The corresponding activation and reaction energies are summarized in Table 2. All energies are given relative to the corresponding reactant structure energies. In Table 3, selected geometrical parameters of the stationary points of all ten PESs are given. In figures and tables, PH and TSH represent the protonated product and transition state species, respectively, while R and TS stand for the corresponding nonprotonated stationary points (Scheme 2).

Our previous calculations¹⁸ predict a very high reaction barrier for the ring-opening reaction of the unsubstituted aziridine ring (**2**) in the presence of two explicit water molecules, representing a low-acidity environment (Table 2, $28\ \text{kcal mol}^{-1}$). In the more acidic environment (modeled by two ammonium ions), the reaction barrier drops to $14\ \text{kcal mol}^{-1}$ due to protonation of the TS structure (TSH, Table 2). In the case of the CHO -substituted aziridine (**3**) (both environments), the transition state remains unprotonated in the presence of water and of ammonium ions, but the barrier heights are nonetheless quite low with 13 and $14\ \text{kcal mol}^{-1}$, respectively (Table 2). The substituents treated in the present work have the same impact on the inhibition reaction energy profile. Characteristic for all PESs in Figures 2–6 is that none of the transition state structures gets protonated, either by water or by ammonium ions (see also

SCHEME 2: Model Reaction of the Alkylation of Methyl Thiolate by an N-Substituted Aziridine Ring Computed in the Present Work^a

^a R stands for reactants, TS for transition state, TSH for protonated transition state, P for nonprotonated product, and PH for protonated product structure.

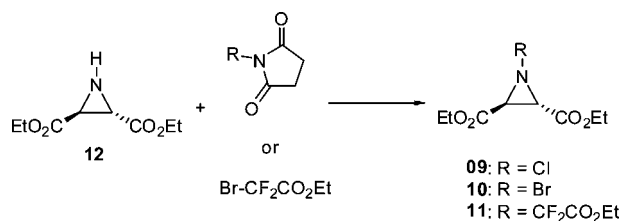
SCHEME 3: Syntheses of Inhibitors 9, 10, and 11

Table 2). If ammonium ions are employed as solvent molecules, a protonation takes place after the TS. For more basic environments modeled by two explicit water molecules the substituted aziridine ring remains unprotonated along the whole reaction course. The reaction barriers drop to 13–16 kcal mol⁻¹ (inhibitors 4–8, Table 2), which is similar to the value obtained for X = CHO (inhibitor 3). With chlorine (4) and bromine (5) atoms as substituents, the energy barrier in water is 16 kcal mol⁻¹ while 15 kcal mol⁻¹ is predicted in the presence of ammonium. The same activation energies are seen with the CF₂H substituent (7) in both solvents. The C₆H₄NO₂ moiety (8) leads to an energy barrier of 14 kcal mol⁻¹ in both solvation environments. The CF₃ substituent (6) shows the greatest influence on the reaction kinetics with reaction barriers of 13 and 12 kcal mol⁻¹ for water and ammonium, respectively. The reason for this decrease in activation energies, and hence acceleration of the irreversible inhibition step, is the electron-withdrawing effect of the substituents. It lowers the basicity of the aziridine N-atom due to the corresponding -I effects. A comparison of these results with previous ones shows that -I effects can influence the kinetics of the reaction in the same magnitude as -M effects. As a consequence of the electron-withdrawing effect of the substituent charge accumulated on the N-atom during the reaction is partially transferred to the substituent, for example, the CF₃- group, making the nitrogen moiety a much better leaving group in the S_N2 reaction. The stabilization of the negative charge on the opening ring is reflected in nonprotonated TS structures of N-substituted rings even in cases where NH₄⁺ ions serve as explicit solvent molecules. Even in cases where a protonated TS (denoted TSH) could be found for a N-substituted system (bromine and chlorine substituents), this state is actually 2 kcal mol⁻¹ higher in energy than the nonprotonated transition state (denoted TS). For comparison, the unsubstituted aziridine ring (2) experiences protonation under such circumstances. This underlines the degree of charge stabilization and explains why a change in the proton-donor affinity of the surroundings (water vs ammonium ions) does not much influence the kinetics of the reaction. The increase of the reaction barrier due to the presence

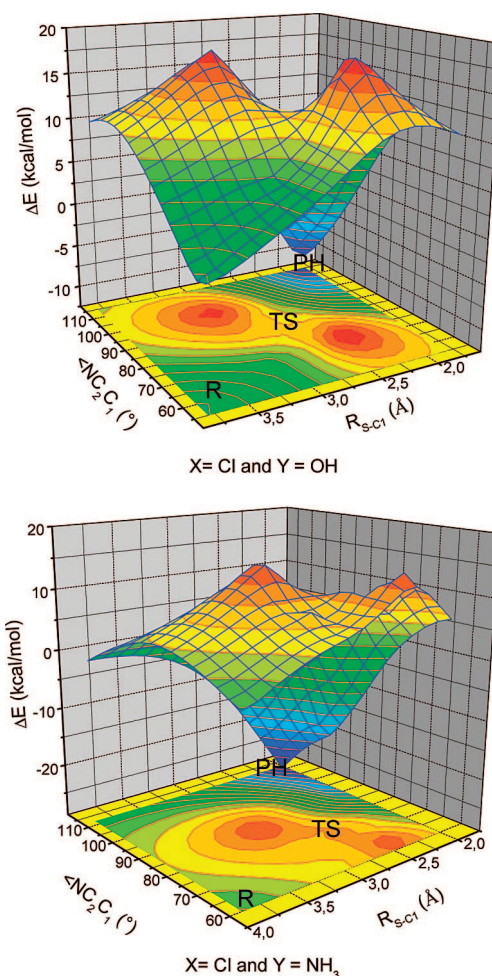


Figure 2. Potential energy surfaces (PES) computed for the systems containing Cl as N-substituent (4) with two explicit water molecules (top) or two explicit ammonium ions (bottom) as solvent.

of water as solvent is 1 kcal mol⁻¹ at most (Table 2). A difference between the systems solvated in water and those solvated in ammonium appears only at the end of the reaction path in the product structures. The reactions with NH₄⁺ are thermodynamically preferred, since protonation of the product lowers the reaction energy by 13–20 kcal mol⁻¹. This is consistent with the basicity of the nonprotonated product and the higher acidity of ammonium in comparison to water.

The strengths of the -M or -I effects are also reflected in the existence of the nonprotonated product structures when the solvent is represented by two water molecules. With X = CHO (3), Br (5), and Cl (4), the nonprotonated products are 2 kcal

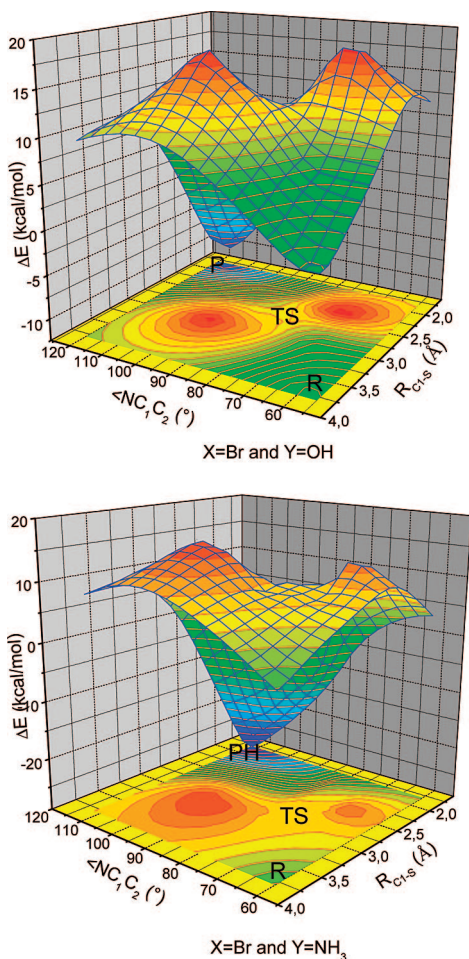


Figure 3. Potential energy surfaces (PES) computed for the systems containing Br as N-substituent (**5**) with two explicit water molecules (top) or two explicit ammonium ions (bottom) as solvent.

mol^{-1} more stable than their protonated counterparts. Calculations with an unsubstituted aziridine ring and water molecules as explicit solvent only yield protonated PH structures (Table 2) indicating that the unprotonated counterparts are much higher in energy or perhaps do not even represent minima on the PES. Comparing the substituted aziridines (**4**–**8**) with the nonsubstituted counterpart ($X = \text{H}$, **2**) their enhanced alkylation abilities are obvious for alkaline media. With decreasing pH values the differences should become smaller.

To verify the theoretical predictions compounds **9**, **10**, and **11**, analogues of the model compounds **4**, **5**, **6**, and **7**, were synthesized and tested as described above. A first screening with a concentration of $100 \mu\text{M}$ confirmed significant inhibitory power of all three aziridine derivatives. The pseudo first-order rate constant k_{obs} was measured in continuous assays. The progress curves for the time-dependent inhibition of falcipain 2 are depicted exemplarily for an assay with inhibitor **11** in Figure 6. The individual inhibition constants k_i , K_i , and $k_{2\text{nd}}$ (see Figures 7 and 8) for inhibitors **9**, **10**, and **11** are presented in Table 4.

The $k_{2\text{nd}}$ values for inhibition of cathepsin L by the N-unsubstituted aziridine-2,3-dicarboxylate **12** and the N-alkyl-derivative **13** are included for comparison.⁴⁸

The data clearly states the improved inhibition potency of the new inhibitors **9**, **10**, and **11** compared to compounds **12** and **13**. The most potent inhibitor with respect to the $k_{2\text{nd}}$ value is compound **9**, offering a 2300-fold increase in inhibition (Table

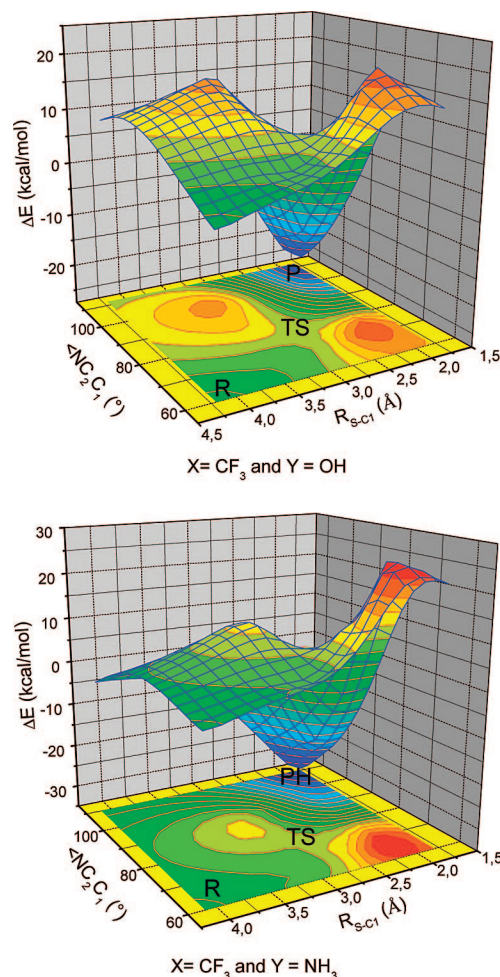


Figure 4. Potential energy surfaces (PES) computed for the systems containing CF_3 as N-substituent (**6**) with two explicit water molecules (top) or two explicit ammonium ions (bottom) as solvent.

TABLE 2: Relative Energies (in kcal mol^{-1}) Describing the Influence of the Substituents and Explicit Solvent Molecules on the Reaction Profiles of the Ring-Opening Reaction

inhibitor	X	Y = OH				Y = NH_3			
		TS	TSH	P	PH	TS	TSH	P	PH
2	H^a	28			6	14			-24
3	CHO^a	14		-25	-23	13			-41
4	Cl	16		-12	-10	15	17		-31
5	Br	16		-12	-10	15	17		-31
6	CF_3	13		-23		12			-36
7	CF_2H	16		-17		15			-34
8	$\text{C}_6\text{H}_4\text{NO}_2$	14		-25		14	12		-38

^a The results are taken from ref 18.

4) compared to the unsubstituted inhibitor **12**. Weaker, but still significantly enhanced inhibitory potencies are shown by inhibitors **10** and **11** (1000-fold and 540-fold increase in inhibition). A comparison of the k_i and K_i values of inhibitors **9**, **10**, and **11** provides a more detailed picture. Inhibitor **9** possesses the smallest dissociation constant K_i , that is, it fits best into the binding pocket of the enzyme. This may result since chlorine, which is quite space filling and lipophilic, favorably interacts with the protein environment. The small dissociation constant mainly determines the high $k_{2\text{nd}}$ -value while according to measured k_i the alkylation reaction itself is slowest for inhibitor **9**. Compound **11** exhibits the highest k_i -value but due to its high K_i -value it exhibits the lowest $k_{2\text{nd}}$ -value.

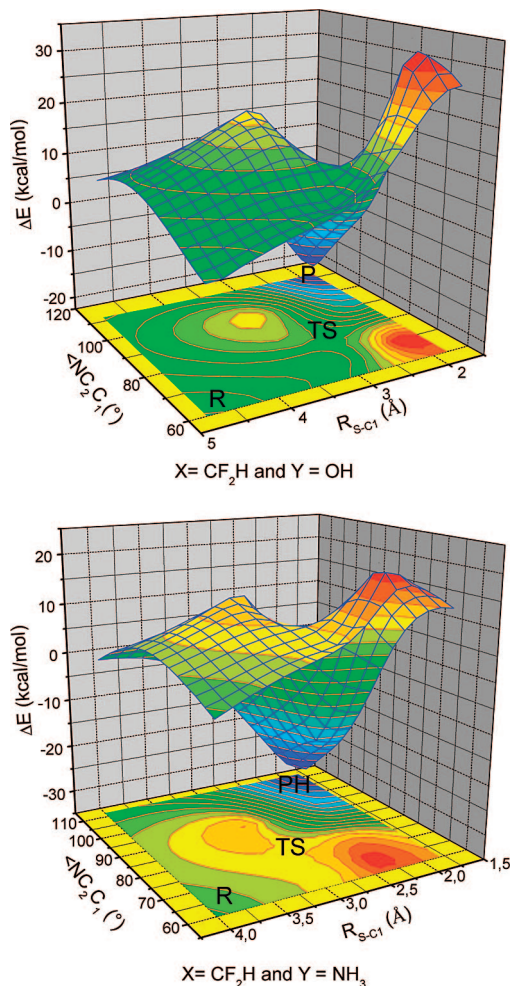


Figure 5. Potential energy surfaces (PES) computed for the systems containing CF₂H as N-substituent (**7**) with two explicit water molecules (top) or two explicit ammonium ions (bottom) as solvent.

The calculated reaction barriers nicely correlate with the k_i values. The tested inhibitor **11** that undergoes ring-opening at the highest rate in enzymatic assays corresponds to the substituent that yields the lowest reaction barrier (**6**). To ascertain that the inhibition mechanism is the irreversible alkylation of the cysteine residue of the protease's active site under ring-opening of the new inhibitors, we performed model reactions of **11** with 4-methoxy thiophenolate as described above.¹⁸ Each model reaction was followed for two days by NMR spectroscopy. In both, the pseudo first-order and the second-order experiments, **11** reacted readily with the provided nucleophile. Conversions to the ring-opening product (identified by the increasing signals of the thiolate-aziridine adduct at $\delta = 7.34$ ppm and the decreasing singlet of the ring protons at $\delta = 3.57$ ppm) of over 50% within one day were detected. As reported previously, the N-unsubstituted aziridine **12** only yielded low concentrations of ring-opening product after 4 days.¹⁸ For the model reaction with inhibitor **11**, both the second-order k_2 and the pseudo first-order rate constants k_2' could be determined graphically from plots of concentrations of the aziridine or aziridine-thiol-adduct vs time. They resulted to $k_2 = 1.56 \text{ M}^{-1} \text{ min}^{-1}$ and $k_2' = 1.44 \cdot 10^{-3} \text{ min}^{-1}$, respectively. These values are typical for the rate constants of ring-opening reactions of epoxides with thiols.⁴⁷ The findings show that the introduction of an electron-withdrawing group at the aziridine-nitrogen greatly accelerates the inhibition reaction. The results confirm

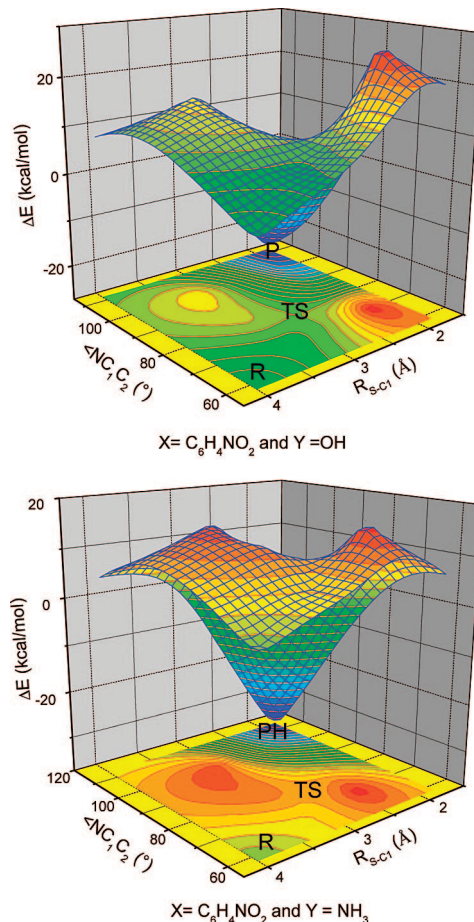


Figure 6. Potential energy surfaces (PES) computed for the systems containing C₆H₄NO₂ as N-substituent (**8**) with two explicit water molecules (top) or two explicit ammonium ions (bottom) as solvent.

our predictions that such aziridines are similar to epoxides regarding the rates of the inhibition reaction.

Summary

Compared to their oxygen analogues, N-unsubstituted aziridines are less potent inhibitors and show lower alkylating rate constants. However, they feature an additional site for substitution at the nitrogen center that makes them an attractive class of substances, offering many possibilities to modulate the inhibitor's reactivity. In the present paper, substitution at this site is exploited for the design of aziridine-based electrophilic warheads with increased inhibition potency. In a first step, the expected influence of electron-withdrawing substituents (CHO, Cl, Br, CF₃, CF₂H, and C₆H₄NO₂) on the inhibition potency is tested by quantum chemical calculations of the ring-opening reaction of the substituted aziridine with methylthiolate. The influence of the acidity of the surroundings is probed by adding either two water molecules ($\text{p}K_{\text{a}} \approx 15$) or two ammonium ions ($\text{p}K_{\text{a}} \approx 9.3$). Additional solvent effects were mimicked by the continuum solvent model using a dielectric constant of $\epsilon = 78.39$. Insights into kinetics and thermodynamics of the ring opening reaction, which represents the irreversible alkylation step of the overall inhibition mechanism, are obtained through two-dimensional potential energy surfaces. The calculations are performed for six different substituents (X = CHO, Cl, Br, CF₃, CF₂H, and C₆H₄NO₂), which are compared with the unsubstituted aziridine (X = H).

The computed reaction barriers of the substituted aziridines range from 13–16 kcal mol⁻¹ that represents reductions of up

TABLE 3: Geometry Parameters for Systems Containing Different N-Substituents (X) and Explicit Solvent Molecules (Y) for the Stationary Points along the Reaction Path

system		$\angle \text{NC}_2\text{C}_1$	RS-C_1	$\text{RC}_1\text{-C}_2$	RN-C_1	RN-C_2	RN-YH	RN-X
X/Y		($^\circ$)	(\AA)	(\AA)	(\AA)	(\AA)	(\AA)	(\AA)
Cl/OH	R	59.9	3.767	1.492	1.493	1.498	1.900	1.868
	TS	80.4	2.666	1.469	1.906	1.484	1.800	1.862
	P	115.0	1.874	1.548	2.530	1.451	1.611	1.929
Cl/NH ₃	R	60.1	3.847	1.493	1.497	1.497	1.789	1.845
	TS	79.6	2.660	1.471	1.890	1.483	1.659	1.848
	PH	111.8	1.863	1.534	2.485	1.478	1.052	1.858
Br/OH	R	59.7	3.701	1.492	1.489	1.498	1.891	2.036
	TS	80.3	2.642	1.469	1.904	1.483	1.793	2.006
	P	115.1	1.874	1.548	2.532	1.452	1.625	2.064
Br/NH ₃	R	59.9	3.771	1.492	1.492	1.496	1.773	1.999
	TS	79.4	2.645	1.471	1.887	1.482	1.636	1.992
	PH	111.8	1.864	1.534	2.496	1.480	1.052	2.001
CF ₃ /OH	R	60.2	4.146	1.490	1.499	1.497	1.967	1.410
	TS	75.4	2.773	1.469	1.808	1.487	1.871	1.374
	P	110.2	1.869	1.543	2.475	1.473	1.764	1.296
CF ₃ /NH ₃	R	60.4	4.028	1.488	1.504	1.502	1.881	1.417
	TS	75.5	2.780	1.468	1.811	1.490	1.740	1.382
	PH	109.4	1.864	1.539	2.469	1.486	1.051	1.372
CF ₂ H/OH	R	59.9	4.685	1.495	1.491	1.492	1.927	1.420
	TS	76.8	2.741	1.471	1.835	1.484	1.814	1.383
	P	111.5	1.870	1.545	2.495	1.472	1.724	1.300
CF ₂ H/NH ₃	R	60	3.994	1.493	1.495	1.498	1.824	1.428
	TS	77.4	2.738	1.472	1.849	1.486	1.671	1.392
	PH	110.2	1.865	1.541	2.476	1.478	1.042	1.368
C ₆ H ₄ NO ₂ /OH	R	59.5	3.928	1.504	1.481	1.479	1.935	1.406
	TS	74.9	2.766	1.478	1.791	1.469	1.835	1.385
	P	110.8	1.867	1.548	2.482	1.467	1.757	1.332
C ₆ H ₄ NO ₂ /NH ₃	R	59.9	3.911	1.500	1.490	1.485	1.802	1.418
	TS	75.1	2.775	1.475	1.798	1.474	1.674	1.395
	PH	112.1	1.864	1.548	2.500	1.466	1.042	1.359

to 15 kcal mol⁻¹ with respect to the nonprotonated transition state of the unsubstituted aziridine. For more acidic environments for which the reaction is expected to run over protonated transition states, the differences are smaller (≈ 2 kcal mol⁻¹). These findings generalize our previous results found for N-formylated aziridines and show that inductive effects can influence the kinetics of the reactions in the same magnitude as mesomeric effects. This indicates that the new warheads should be very efficient in neutral and alkaline media. For acidic environments smaller but still significant differences are expected. The theoretical predictions could experimentally be verified by the syntheses and the testings of the three new compounds **9** (X = Cl), **10** (X = Br), and **11** (X = CF₂CO₂Et).

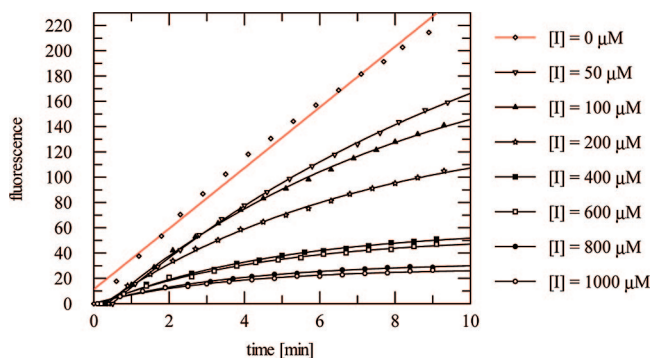


Figure 7. Progress curves for the time-dependent inhibition of falcipain 2 by **11**. The data were fitted to the equation $[\text{fluorescence}] = A(1 - \exp(-k_{\text{obs}}t)) + B$ to obtain the pseudo first-order rate constants of inhibition k_{obs} in dependence of the inhibitor concentrations $[I]$ by nonlinear regression analysis using the enzyme kinetics program GraFit 5.0.13, Erithacus Software Ltd., 2006.

On the basis of the $k_{2\text{nd}}$ values they display an up to 2300-fold increase in inhibition potency compared to the unsubstituted inhibitor **12**. In line with the theoretical predictions for acidic media this increase results not only from an acceleration of the alkylation step (k_i value). Especially for X = Cl the enhancement of the inhibition potency also results from an improved fit into the enzyme (K_i value). The most promising substituents are CF₂H or CF₂COOEt. They allow further derivatization of the building block, for example, insertion of peptidomimetic side

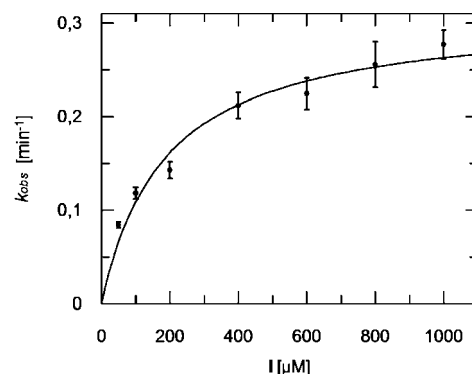


Figure 8. $k_{\text{obs}}/[I]$ diagram of the time-dependent inhibition of falcipain 2 by **11**. The data were fitted to the equation $[k_{\text{obs}} = k_i[I]/(K_i^{\text{app}} + [I])]$ to obtain the apparent dissociation constant K_i^{app} and the first-order rate constant of inhibition k_i by nonlinear regression analysis using the enzyme kinetics program GraFit 5.0.13, Erithacus Software Ltd., 2006. The K_i^{app} value was corrected to zero substrate concentration by the term $(1 + [S]/K_m)$ in equation $K_i = K_i^{\text{app}}/(1 + [S]/K_m)$ with the substrate concentration $[S] = 50 \mu\text{M}$ and the Michaelis constant $K_m = 21.5 \mu\text{M}$. The second-order rate constant $k_{2\text{nd}} = k_i/K_i$ was directly calculated from the individual constants.

TABLE 4: Inhibition of Falcipain 2 by Aziridine Derivatives^a

inhibitor	k_i (min ⁻¹)	K_i (μM)	k_{2nd} (M ⁻¹ min ⁻¹)
9	0.10	4.5	25,641
10	0.15	15.8	11,029
11	0.23	38.4	5,974
12			11 ^b
13			8 ^b

^a Values are mean values of 2–4 independent assays, standard deviations are less than 10% in all cases. ^b Inhibition of cathepsin L, taken from ref 48.

chains that further improve the reversible interactions between inhibitor and enzyme. Furthermore, the results underline that in the case of the N-formyl aziridine, which surprisingly did not display enhanced k_i values, other reaction pathways (e.g., attack at the carbonyl carbon) may indeed be involved in the inhibition mechanism.

Acknowledgment. Financial support by the DFG (Deutsche Forschungsgemeinschaft) in the framework of the SFB630 is gratefully acknowledged. We gratefully thank Professor Dr. P. Rosenthal, University of California, San Francisco, CA, for supplying us with the plasmid for recombinant FP-2 from *P. falciparum*.

Supporting Information Available: General information for the experiments, synthesis of diethyl aziridine-2,3-dicarboxylate, inhibitor 9–11, fluorometric enzyme assays, Cartesian coordinates of optimized QM regions, and correlation between distances and barriers. This material is available free of charge via the Internet at <http://pubs.acs.org>.

References and Notes

- (1) World Health Organization Report on Infectious Diseases: <https://www.who.int/infectious-disease-report/index.html>.
- (2) (a) Rawlings, N. D.; Morton, F. R.; Kok, C. Y.; Kong, J.; Barrett, A. J. *Nucleic Acids Res.* **2008**, *36*, D320–D325. (b) MEROPS, the Peptidase Database, Release 8.3, 2008. <http://merops.sanger.ac.uk/>.
- (3) Leung-Toung, R.; Li, W. R.; Tam, T. F.; Karimian, K. *Curr. Med. Chem.* **2002**, *9*, 979–1002.
- (4) Bromme, D.; Kaleta, J. J. *Curr. Pharm. Design.* **2002**, *8*, 1639–1658.
- (5) Turk, B.; Turk, D.; Turk, V. *Biochim. Biophys. Acta* **2000**, *1477*, 98–111.
- (6) Lecaille, F.; Kaleta, J.; Brömme, D. *Chem. Rev.* **2002**, *102*, 4459–4488.
- (7) Rawlings, N. D.; Tolle, D. P.; Barrett, A. J. *Nucleic Acids Res.* **2004**, *32*, D160–D164.
- (8) Mladenovic, M.; Fink, R. F.; Thiel, W.; Schirmeister, T.; Engels, B. *J. Am. Chem. Soc.* **2008**, *130*, 8696–8705.
- (9) Hanada, K.; Tamai, M.; Yamagishi, M.; Ohmura, S.; Sawada, J.; Tanaka, I. *Agric. Biol. Chem.* **1978**, *42*, 523–528.
- (10) Powers, J. C.; Asgian, J. L.; Ekici, O. D.; James, K. E. *Chem. Rev.* **2002**, *102*, 4639–4750.
- (11) Schirmeister, T. *J. Med. Chem.* **1999**, *42*, 560–572.
- (12) Vicik, R.; Busemann, M.; Gelhaus, C.; Stiefl, N.; Scheiber, J.; Schmitz, W.; Schulz, F.; Mladenovic, M.; Engels, B.; Leippe, M.; Baumann, K.; Schirmeister, T. *ChemMedChem* **2006**, *1*, 1126–1141.

- (13) Schulz, F.; Gelhaus, C.; Degel, B.; Vicik, R.; Heppner, S.; Breuning, A.; Leippe, M.; Gut, J.; Rosenthal, P. J.; Schirmeister, T. *ChemMedChem* **2007**, *2*, 1214–24.
- (14) Gelhaus, C.; Vicik, R.; Hilgenfeld, R.; Schmidt, C. L.; Leippe, M.; Schirmeister, T. *Biol. Chem.* **2004**, *385*, 435–438.
- (15) Gelhaus, C.; Vicik, R.; Schirmeister, T.; Leippe, M. *Biol. Chem.* **2005**, *386*, 499–502.
- (16) Helten, H.; Schirmeister, T.; Engels, B. *J. Org. Chem.* **2005**, *70*, 233–237.
- (17) Helten, H.; Schirmeister, T.; Engels, B. *J. Phys. Chem.* **2004**, *108*, 76917701.
- (18) Vicik, R.; Helten, H.; Schirmeister, T.; Engels, B. *ChemMedChem* **2006**, *1*, 1021–1028.
- (19) Sijwali, P. S.; Brinen, L. S.; Rosenthal, P. J. *Protein Expression Purif.* **2001**, *22*, 128–34.
- (20) Smith, R. A.; Copp, L. J.; Donnelly, S. L.; Spencer, R. W.; Krantz, A. *Biochemistry* **1988**, *27*, 6568–6573.
- (21) Banks, H. D. *J. Org. Chem.* **2006**, *71*, 8089–8097.
- (22) Banks, H. D. *J. Org. Chem.* **2008**, *73*, 2511–2517.
- (23) Mladenovic, M.; Junold, K.; Fink, R. F.; Thiel, W.; Schirmeister, T.; Engels, B. *J. Phys. Chem. B* **2008**, *112*, 5458–69.
- (24) Mladenovic, M.; Ansorg, K.; Fink, R. F.; Thiel, W.; Schirmeister, T.; Engels, B. *J. Phys. Chem. B* **2008**, *112*, 11798–11808.
- (25) Mladenovic, M.; Schirmeister, T.; Thiel, S.; Thiel, W.; Engels, B. *ChemMedChem* **2007**, *2*, 120.
- (26) Cavalli, A.; Carloni, P.; Recanatini, M. *Chem. Rev.* **2006**, *106*, 3497.
- (27) Klamt, A.; Schuurmann, G. J. *J. Chem. Soc., Perkin. Trans. 2* **1993**, *2*, 799.
- (28) (a) Vahtras, O.; Almlöf, J.; Feyereisen, M. W. *Chem. Phys. Lett.* **1993**, *213*, 514. (b) Eichkorn, K.; Treutler, O.; Öhm, H.; Häser, M.; Ahlrichs, R. *Chem. Phys. Lett.* **1995**, *242*, 652.
- (29) (a) Becke, A. D. *Phys. Rev. A* **1988**, *38*, 3098. (b) Lee, C.; Yang, W.; Parr, R. G. *Phys. Rev. B* **1988**, *37*, 785.
- (30) Schäfer, A.; Huber, C.; Ahlrichs, R. *J. Chem. Phys.* **1997**, *100*, 5829.
- (31) Adam, W.; Bottke, N.; Engels, B.; Krebs, O. *J. Am. Chem. Soc.* **2001**, *123*, 5542.
- (32) Schlund, S.; Mladenovic, M.; Basilio Janke, E. M.; Engels, B.; Weisz, K. *J. Am. Chem. Soc.* **2005**, *127*, 16151.
- (33) Hupp, T.; Sturm, C.; Basilio Janke, E. M.; Perez Cabre, M.; Weisz, K.; Engels, B. *J. Phys. Chem.* **2005**, *109*, 1703.
- (34) Engels, B.; Schoeneboom, J. C.; Munster, A. F.; Groetsch, S.; Christl, M. *J. Am. Chem. Soc.* **2002**, *124*, 287.
- (35) Suter, H. U.; Plesse, V.; Ernzerhof, M.; Engels, B. *Chem. Phys. Lett.* **1994**, *230*, 398.
- (36) Suter, H. U.; Engels, B. *J. Chem. Phys.* **1994**, *100*, 2936.
- (37) Engels, B. *Theo. Chim. Acta* **1993**, *86*, 429.
- (38) Schmittel, M.; Steffen, J. P.; Engels, B.; Lennartz, C.; Hanrath, M. *Angew. Chem., Int. Ed.* **1998**, *37*, 2371.
- (39) Engels, B.; Peyerimhoff, S. D. *J. Phys. Chem.* **1989**, *93*, 4462.
- (40) Engels, B.; Hanrath, M.; Lennartz, C. *Comput. Chem. (Oxford, U.K.)* **2001**, *25*, 15.
- (41) Musch, P. W.; Engels, B. *J. Am. Chem. Soc.* **2001**, *123*, 5557.
- (42) Ahlrichs, R.; Bär, M.; Baron, H.-P.; Bauernschmitt, R.; Bockner, S.; Ehring, M.; Eichkorn, K.; Elliott, S.; Furch, F.; Haase, F.; Häser, M.; Horn, H.; Huber, C.; Huniar, U.; Kattaneck, M.; Kölmel, C.; Kollwitz, M.; May, K.; Ochsenfeld, C.; Öhm, H.; Schäfer, A.; Schneider, U.; Treutler, O.; v. Arnim, M.; Weigend, F.; Weis, P.; Weiss, H. *TURBOMOLE Version 5.6*; Universität Karlsruhe: Karlsruhe, Germany, 1988.
- (43) Breuning, A.; Vicik, R.; Schirmeister, T. *Tetrahedron: Asymmetry* **2003**, *14*, 3301–3312.
- (44) Shustov, G. V.; Kachanov, V.; Korneev, V. A.; Kostyanovsky, R. G.; Rauk, A. *J. Am. Chem. Soc.* **1993**, *115*, 10267–10274.
- (45) Tian, W.-X.; Tsou, C.-L. *Biochemistry* **1982**, *21*, 1028–1032.
- (46) *GraFit 5.0.13*; Software Ltd.: London, 2006.
- (47) Bihovsky, R. *J. Org. Chem.* **1992**, *57*, 1029–1031.
- (48) Schirmeister, T.; Peric, M. *Bioorg. Med. Chem.* **2000**, *8*, 1281–1291.

JP810549N